European Journal of Mechanics / A Solids 111 (2025) 105514

Contents lists available at ScienceDirect

European Journal of Mechanics / A Solids

journal homepage: www.elsevier.com/locate/ejmsol

Full length article

Beams on elastic foundation: A variable reduction approach for nonlinear contact problems

Giorgio Previati [*], Federico Ballo, Pietro Stabile

Department of Mechanical Engineering, Politecnico di Milano, Via La Masa 1, Milano, 20156, Italy

A R T I C L E I N F O

Keywords:
Nonlinear elastic foundation
Finite element method
Variable reduction
Independent meshes
Gap modelling

A B S T R A C T

Beams on elastic foundations are applied to a vast number of engineering problems. Several elastic foundation models are available, from the simplest Winkler element with one parameter to complex models with more parameters and nonlinear characteristics. Analytical and numerical approaches have been developed in the literature for the solution of this problem, often specialized for a particular application. In this paper, a novel numerical approach that can be applied to any combination of beam and foundation models is presented. The method is based on independent meshes for the beam and for the foundation. The independent discretization of the foundation opens the possibility to model any kind of foundation behaviour, including nonlinearities, discontinuities and space-dependent properties. The two meshes are then connected by a variable reduction approach, formulated by standard finite element procedures. Such an approach allows to refine the discretization of the foundation without affecting the dimension of the solving system, i.e. with a limited effect on the computational time. Additionally, a relevant advantage of the presented method is that, contrary to most approaches described in the literature, gaps between the beam and the foundation can be straightforwardly included by an energy-based formulation. Examples of applications to linear, nonlinear, and foundation with gaps are reported in the paper. This innovative approach not only simplifies the modelling process but also offers significant computational advantages, making it a versatile and efficient tool for a wide range of engineering applications involving beam–foundation interactions.

1. Introduction

Beams on elastic foundations are widely employed in a broad variety of engineering fields. In structural and civil engineering, the design and construction of safe and efficient buildings and structures require an accurate modelling of structure–soil interaction in the foundation system (Tiwari and Kuppa, 2014; Singh and Jha, 2013; Madhira et al., 2016; Harden and Hutchinson, 2009). In tunnels and buried pipelines design (Xiong et al., 2023; Dai et al., 2011; Klar et al., 2005), models based on beam on elastic foundation are extensively employed to analyse the structure deformation induced by soil settlement.

The behaviour of railway tracks during the passage of the train is commonly studied by means of beam on elastic foundation models (Cojocaru et al., 2003; Lamprea-Pineda et al., 2022). In the automotive field, tyre deflection and tyre-rim interaction mechanisms can be effectively modelled with curved beams on elastic foundation (Kim et al., 2008; Ballo et al., 2015, 2016, 2018).

In the design of cold rolling mill plants, roll-gap profile can be estimated by means of beam elements describing the transverse deformation of the roll axes connected by foundation elements modelling the contact interaction among the rolls (Malik and Grandhi, 2008).

The earliest foundation model was developed by Winkler in 1868 (Winkler, 1868), who provided the simplest representation of a continuous elastic foundation, which assumes a sequence of independent linear springs. The pressure on the foundation surface is proportional to the surface deflection and the relation is given by the foundation modulus. The Winkler foundation was soon improved by the addition of a viscous element with different arrangements, resulting in novel viscoelastic foundation models such as Kelvin–Voigt, Maxwell, Zener, Poynting–Thomson and Burger (Kerr, 1964; Younesian et al., 2019). The main drawback of these models was that the viscoelastic elements of the foundation react independently to the external load, leading to a discontinuous deflection at the border between loaded and unloaded regions (Kerr, 1964; Younesian et al., 2019).

The independent response of the viscoelastic elements is addressed with the addition of an upper layer either in the form of a stretched membrane (Filonenko-Borodich (Kerr, 1964)), or a bending element (Hetényi (Hetenyi, 1946)) or a shear-bearing layer (Pasternak (Pasternak, 1954)). In other cases, such as the Vlasov and Reissner foundation

* Corresponding author.
E-mail address: giorgio.previati@polimi.it (G. Previati).

https://doi.org/10.1016/j.euromechsol.2024.105514
Received 23 May 2024; Received in revised form 25 November 2024; Accepted 26 November 2024
Available online 3 December 2024

models, the problem was approached from a variational continuum perspective (Kerr, 1964; Younesian et al., 2019).

Depending on the type of analysis, more complex models can be found in the literature such as the multi-layered models extensively employed for the vibrational analysis of railway tracks (Lamprea-Pineda et al., 2022; Younesian et al., 2019) or bi-moduli and nonlinear models typically used to account for contact nonlinearities, amplitude dependency response of the foundation and friction (Fallah and Aghdam, 2011; Zhang et al., 2018; Adin et al., 1985; Younesian et al., 2019).

According to the literature four theories are commonly employed to describe the transverse vibration of a beam, namely the Euler–Bernoulli, Rayleigh, shear and Timoshenko (Younesian et al., 2019). In the Euler–Bernoulli theory the sole contribution of the bending moment is considered in the beam deformation. In the Rayleigh model, the effect of the cross-section rotary inertia is included, while in the shear beam model the shear contribution is considered in the beam deformation but the rotary inertia is neglected. Finally, the Timoshenko formulation accounts for both shear deformation and cross-section rotary inertia (Younesian et al., 2019).

From the early 1900s, researchers' efforts have been continuously devoted to the study of beam on elastic foundation systems, combining the mentioned models of beams and elastic foundations either with analytical or numerical approaches (Hetenyi, 1946; Zhaohua and Cook, 1983; Adhikari, 2021; Mourelatos and Parsons, 1987; Chen et al., 2004; Girija Vallabhan and Das, 1991; Bao and Han, 1999; Balabušić et al., 2019; Frydrýek et al., 2013; Onu, 2008; Akhazhanov et al., 2023; Zhang and Fan, 2023). For detailed state of the art papers on the topic, readers should refer to Wang et al. (2005), Younesian et al. (2019).

Moreover, nonlinear models have been widely studied in the literature. For beams, the transverse displacement for large deflections is governed by the one-dimensional von Karman model as shown in Gao (1996), Jain et al. (2018). In Gao (1996), the author introduces a novel nonlinear beam model (Gao beam) to be applied for modelling the behaviour of thick beams under large displacements. In fact, if the beam is quite thick, the stress in the thickness direction cannot be neglected, and the problem is solved by introducing the 2D linear elastic constitutive relation (Gao, 1996; Malekzadeh and Karami, 2008).

Foundation models, on the other hand, are often used to describe contact interaction problems, where the beam can detach from the foundation, giving rise to additional nonlinear effects (Gao, 1996; Gao et al., 2015; Machalová and Netuka, 2017).

In Gao et al. (2015), the authors analyse the behaviour of a largely deformed beam on elastic foundation. In the paper, a Gao beam on a Winkler foundation is considered, and a mathematical formulation of the problem based on a variational approach is provided. Two different problems are analysed, namely the classical foundation, where beam and foundation are firmly connected and the unilateral foundation, where the beam rests on the foundation and normal detachment is allowed. The authors developed a solution strategy based on a mixed hybrid formulation approach (Gao et al., 2015; Brezzi and Fortin, 1991; Machalová and Netuka, 2011a,b, 2018). A decomposition method is employed to define two independent integration domains associated with the beam and the elastic foundation respectively. A linear equality constraint is introduced to link the independent variables and enforce compatibility conditions at the connection between beam and foundation. The classical potential energy minimization problem is transformed into a constrained minimization problem with the introduction of the linear equality, and the resulting problem is finally solved by means of a primal–dual optimization approach. The use of domain decomposition allows for independent meshing and interpolation of the domains of beam and elastic foundation. In the paper numerical examples are solved by using beam elements with cubic shape functions and constant stiffness Winkler foundation elements.

The same authors, in more recent papers, extended their results by including also contact interactions with nonzero initial gap (Machalová and Netuka, 2015) and an axial force acting at the tip of the beam (Radová and Machalová, 2024). Indeed, this topic finds extremely important applications in modelling stitching behaviour between micro-cantilever structures and substrate in MEMS (Micro Electro Mechanical Systems) design (Zhang and Zhao, 2012) or in modelling contact interactions in rolling mills with crown profiles (Malik and Grandhi, 2008; Zhang and Malik, 2018).

Zhang and Murphy address the topic of a finite elastic beam resting on an elastic foundation in two papers (Zhang and Murphy, 2004, 2013). Equilibrium equations and boundary conditions related to a finite Euler–Bernoulli beam loaded with a concentrated force with a nonzero gap distance from a substrate are formulated. A general analytical expression for the solution of the partial differential equation was derived, along with a set of associated unknown constants arising from the analytical integration, to be determined by imposing boundary conditions. Because of the dependency of the contact area from the applied load, the resulting system of equations is nonlinear and has been solved numerically by means of a Newton–Raphson method.

In this paper, a numerical approach for the solution of beams on elastic foundation problems is presented. The method is based on complete independent meshing of beam and elastic foundation domains. This independent discretization of the foundation, with respect to the beam, allows for the modelling of various types of foundation behaviour, including nonlinearities, discontinuities, and spatially varying properties. The two meshes are then linked by a variable reduction approach, allowing for a simple and effective solution of the problem. Differently from Gao et al. (2015), the method relies on standard displacement-based finite element approach, enabling the use with any type of beam and foundation element. In principle, there is no constraint on the type of element to be used for the discretization of the beam or of the foundation. Also, it is possible to use the same element type for the two meshes or different element types.

Additionally, a novel formulation of Winkler's foundation element is adopted by including the nonlinear contact stiffness and initial gap function in the internal work formulation. In this way, both the contact stiffness matrix and the resulting gap force vector can be straightforwardly computed and assembled in the finite element system. As a result, the numerical solution of the system can be obtained using standard techniques, thus simplifying the implementation of the method. Also, being based on the virtual work principle, this approach ensures that the force equilibrium of the solution is satisfied, and no equilibrium iteration is required during the solution.

The paper is organized as follows. In the next section, the problem under consideration is described and formulated. Then, the proposed numerical method for solving the problem is described in details. Firstly, the considered beam formulations are briefly reviewed. Then, the foundation formulation is provided for both linear and nonlinear foundation stiffness, as well as for cases where there is a gap between the beam and the foundation. The variable reduction approach used to solve the numerical system is then explained. Three numerical examples are presented thereafter, followed by the conclusions.

2. Problem formulation

Fig. 1 depicts a beam on an elastic foundation. The beam, with length L, is subjected to a load $f(x)$ and rests on an elastic foundation with spring characteristics described by the function $p(x)$. Additionally, constraints and concentrated loads can also be present. In the paper, a plane problem is considered where x is the axial coordinate of the beam and w is the transverse displacement.

If a simple Euler–Bernoulli beam model is considered, the expression of a beam on an elastic foundation can be written as

$$EIw^{IV}(x) + p(x) = f(x) \qquad \forall x \in [0, L], \tag{1}$$

where E is the elastic modulus of the material, I the moment of inertia of the cross-section, and $f(x)$ the distributed load applied to the

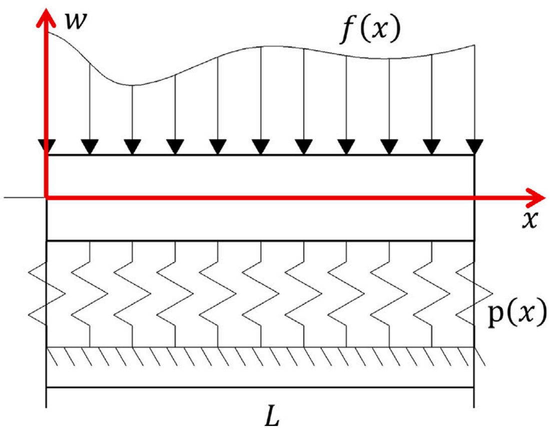

Fig. 1. Beam on elastic foundation.

beam. Eq. (1) represents a Euler–Bernoulli beam on a general elastic foundation.

Different beam formulations can be utilized by replacing the Euler–Bernoulli terms of Eq. (1) ($EIv^{IV}(x)$) with the corresponding terms of the considered formulation. If Timoshenko and Gao (Gao et al., 2015) beams are considered, the equations of a beam on an elastic foundation respectively read

$$EIw^{IV}(x) + \frac{EI}{\kappa AG} w^{II}(x) + p(x) = f(x) \qquad \forall x \in [0, L], \tag{2}$$

$$EIw^{IV}(x) - E\alpha \left(w^{I}(x)\right)^2 w^{II}(x) + p(x) = f(x)\left(1 - \nu^2\right) \qquad \forall x \in [0, L], \tag{3}$$

with A area of the cross-section, G shear modulus of the material, ν the Poisson coefficient of the material, κ shear coefficient of the cross-section, and α is a constant that, for beams with rectangular cross-section of unitary width, can be expressed as (Gao, 1996)

$$\alpha = 3h\left(1 - \nu^2\right), \tag{4}$$

being $2h$ the height of the cross-section (Gao et al., 2015).

Referring to the elastic foundation formulation, several models can be found in the literature (Kerr, 1964; Madhira et al., 2016; Singh and Jha, 2013; Younesian et al., 2019; Lamprea-Pineda et al., 2022). Among all possible formulations, Winkler (Kerr, 1964), Pasternak (Pasternak, 1954), and Hetényi (Hetenyi, 1946) foundations are often employed and are considered in this paper. For these formulations, the mathematical expressions respectively read

$$p(x) = kw(x) \qquad \forall x \in [0, L], \tag{5}$$

$$p(x) = kw(x) - G_h w^{II}(x) \qquad \forall x \in [0, L], \tag{6}$$

$$p(x) = kw(x) - Dw^{IV}(x) \qquad \forall x \in [0, L], \tag{7}$$

where k is the stiffness of the elastic foundation considered in all models, G_h is the stiffness of the shear layer in the Pasternak model, and D is the bending stiffness in the Hetényi model. More details on the different foundation formulations can be found in Kerr (1964), Madhira et al. (2016), Singh and Jha (2013), Younesian et al. (2019), Lamprea-Pineda et al. (2022) and in the references therein.

The different beam and elastic foundation formulations can be combined as required by the considered problem. As the formulation gets more complex, the analytical integration becomes more complicated and only simple load cases can be analysed. Also, in all the considered foundation models the foundation parameters have been considered independent of the beam deflection $w(x)$. However, in several relevant practical applications such parameters depend on the beam deflection or unilateral contacts should be considered. In these cases, the elastic foundation models become nonlinear and an analytical integration may not be possible. For these reasons, in this paper, a numerical approach is considered for the integration of the beam on elastic foundation problem.

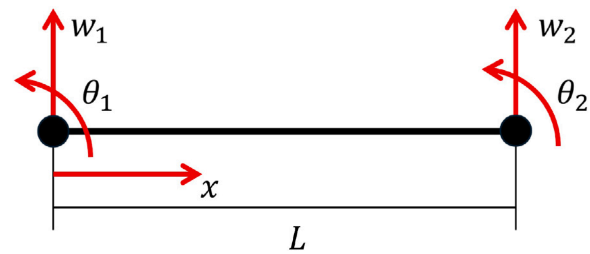

Fig. 2. Scheme of a 4 degrees of freedom beam element.

3. Numerical formulation

For the numerical formulation of the problem, a Finite Element (FE) approach is employed. A beam element is defined for the discretization of the beam, and a foundation element for the elastic foundation. As the foundation element should mimic as accurately as possible the deformation of the beam, a typical choice is to use the same shape functions to describe the displacements of the two elements. In the following, this choice is adopted, even though the presented procedure can be applied in cases where different shape functions are utilized without any modification. As shape functions, the classical Hermite cubic polynomials are considered. Again, the procedure can be applied with any other kind of shape functions complying with the usual requirements for finite element formulation.

Fig. 2 depicts a scheme of the displacements of a standard plane beam element with only transverse deformation and four degrees of freedom (dofs). w_1 and w_2 represent the transverse nodal displacement, θ_1 and θ_2 the nodal rotations, x is the axial coordinate of the element and L the element length. The vector of the nodal displacements can be expressed as

$$\mathbf{d} = \left[\begin{array}{cccc} w_1 & \theta_1 & w_2 & \theta_2 \end{array}\right]^T \tag{8}$$

while the four Hermite cubic polynomials shape functions $\mathbf{N}(x)$ of the element read

$$\mathbf{N}(x) = \left[\begin{array}{cccc} \frac{2x^3}{L^3} - \frac{3x^2}{L^2} + 1, & x - \frac{2x^2}{L} + \frac{x^3}{L^2}, & \frac{3x^2}{L^2} - \frac{2x^3}{L^3}, & \frac{x^3}{L^2} - \frac{x^2}{L} \end{array}\right]. \tag{9}$$

3.1. Beam elements formulation

The FE discretization of Euler–Bernoulli (Eq. (1)) and Timoshenko (Eq. (2)) beams by means of Hermite cubic polynomials is a widely known approach. For the sake of readability, the expressions of the corresponding stiffness matrices $\mathbf{K_B}$ (stiffness matrix of the Euler–Bernoulli beam) and $\mathbf{K_T}$ (stiffness matrix of the Timoshenko beam) are provided in Appendix A.

The FE modelling of the Gao beam (Eq. (3)) can be obtained as follows. Let us consider the shape functions in Eq. (9). By assuming $w^I(x) = \mathbf{N}(x)^I\,\mathbf{d}$, the stiffness matrix of the Gao beam can be computed as (Gao et al., 2015)

$$\mathbf{K_G} = EI\int_0^L \mathbf{N}(x)^{II^T}\mathbf{N}(x)^{II}\,dx + \frac{E\alpha}{3}\int_0^L \left(\mathbf{N}(x)^I\,\mathbf{d}\right)^2 \mathbf{N}(x)^{I^T}\mathbf{N}(x)^I\,dx. \tag{10}$$

The first term of Eq. (10) is equal to the stiffness matrix of a Euler–Bernoulli beam and is reported in Appendix A. The second term is nonlinear as is function of the nodal displacement. This term can be analytically integrated leading to complicated formulas, reported in Appendix B for readability.

3.2. Elastic foundation elements formulation

When implementing a finite element solution for a beam on elastic foundation, the stiffness matrix of the beam element is modified to account for the stiffening effect of the foundation. As pointed out in Zhaohua and Cook (1983), the resulting stiffness matrix is the sum of the stiffness matrix of the beam element and of a stiffness matrix derived from the expression for the elastic foundation and for the considered shape functions. In this paper, as the scope is the creation of two different meshes for the discretization of the beam and of the elastic foundation, the two contributions are kept separated. Therefore, the expression of the foundation element refers to the formulation of the stiffness matrix contribution related to the sole elastic foundation. This stiffness matrix can be then assembled in the solving system, as will be shown in Section 4.

For the numerical implementation of the elastic foundation elements, the same beam element with two nodes and four dofs considered for the beam models and depicted in Fig. 2, with the nodal displacements defined in Eq. (8), and the shape functions in Eq. (9) is assumed. It should be remarked that the choice of the shape function leads to the particular expressions of the matrices derived in the remainder of the paper, but the presented method can be applied to any other suitable set of shape functions.

3.2.1. Linear case: bilateral contact and constant elastic foundation parameters

Firstly, the simplest case of bilateral foundation, i.e. an elastic foundation that reacts in both compression and tension, with constant foundation parameters, is considered. This represents the only case in which the elastic foundation is linear. If the beam formulation is also linear, a linear system can be obtained.

For this case, the computation of the stiffness matrices of the considered foundation formulations is straightforward and can be derived by considering the strain energy function of the elastic foundation. For the Winkler foundation, the strain energy function can be computed by considering a simple spring ($U = \frac{1}{2} k w(x)^2$), and the stiffness matrix reads

$$\mathbf{K_{fW}} = k \int_0^{L_f} \mathbf{N}^T(x)\,\mathbf{N}(x)\,dx = k \begin{bmatrix} \frac{13\,L_f}{35} & \frac{11\,L_f^2}{210} & \frac{9\,L_f}{70} & -\frac{13\,L_f^2}{420} \\ \frac{11\,L_f^2}{210} & \frac{L_f^3}{105} & \frac{13\,L_f^2}{420} & -\frac{L_f^3}{140} \\ \frac{9\,L_f}{70} & \frac{13\,L_f^2}{420} & \frac{13\,L_f}{35} & -\frac{11\,L_f^2}{210} \\ -\frac{13\,L_f^2}{420} & -\frac{L_f^3}{140} & -\frac{11\,L_f^2}{210} & \frac{L_f^3}{105} \end{bmatrix}, \tag{11}$$

where L_f indicates the length of the foundation mesh element. In case of the Pasternak foundation element, the stiffness matrix consists of two parts. The first part is the stiffness matrix of the Winkler foundation element. The second part can be computed by considering that the strain energy of the second term of Eq. (6) is given by shear deformation ($U = \frac{1}{2} G_h \left(\frac{dw(x)}{dx}\right)^2$) (Zhaohua and Cook, 1983). The stiffness matrix, therefore, reads

$$\mathbf{K_{fP}} = k \int_0^{L_f} \mathbf{N}^T(x)\,\mathbf{N}(x)\,dx + G_h \int_0^{L_f} \mathbf{N}^I(x)^T \mathbf{N}^I(x)\,dx = \mathbf{K_{fW}} + G_h \begin{bmatrix} \frac{6}{5\,L_f} & \frac{1}{10} & -\frac{6}{5\,L_f} & \frac{1}{10} \\ \frac{1}{10} & \frac{2\,L_f}{15} & -\frac{1}{10} & -\frac{L_f}{30} \\ -\frac{6}{5\,L_f} & -\frac{1}{10} & \frac{6}{5\,L_f} & -\frac{1}{10} \\ \frac{1}{10} & -\frac{L_f}{30} & -\frac{1}{10} & \frac{2\,L_f}{15} \end{bmatrix}. \tag{12}$$

Similarly, for the Hetényi foundation element, the first term of the stiffness matrix is the stiffness matrix of the Winkler element, while the second term can be computed by considering the strain energy associated with bending deformation ($U = \frac{1}{2} D \left(\frac{d^2 w(x)}{dx^2}\right)^2$). The stiffness matrix thus results

$$\mathbf{K_{fH}} = k \int_0^{L_f} \mathbf{N}^T(x)\,\mathbf{N}(x)\,dx + D \int_0^{L_f} \mathbf{N}^{II}(x)^T \mathbf{N}^{II}(x)\,dx = \mathbf{K_{fW}} + D \begin{bmatrix} \frac{12}{L_f^3} & \frac{6}{L_f^2} & -\frac{12}{L_f^3} & \frac{6}{L_f^2} \\ \frac{6}{L_f^2} & \frac{4}{L_f} & -\frac{6}{L_f^2} & \frac{2}{L_f} \\ -\frac{12}{L_f^3} & -\frac{6}{L_f^2} & \frac{12}{L_f^3} & -\frac{6}{L_f^2} \\ \frac{6}{L_f^2} & \frac{2}{L_f} & -\frac{6}{L_f^2} & \frac{4}{L_f} \end{bmatrix}. \tag{13}$$

3.2.2. Nonlinear case: unilateral contact or nonlinear elastic foundation parameters

In the previous subsection, the case of linear elastic foundation elements has been discussed. However, nonlinearities often arise. In most applications, the elastic foundation is unilateral, i.e. the foundation reacts only in compression. In some cases, the foundation parameters could also depend on the displacements.

Firstly, the case of unilateral contact with constant foundation parameters is considered. For the three considered foundation formulations, given the compression of the foundation element when the displacement is negative ($w(x) \le 0$), the parameters can be defined as follows.

$$k(x) = \begin{cases} 0 & if \;\; w(x) > 0 \\ k & if \;\; w(x) \le 0 \end{cases} \qquad \forall x \in \left[0, L_f\right], \tag{14}$$

$$G_h(x) = \begin{cases} 0 & if \;\; w(x) > 0 \\ G_h & if \;\; w(x) \le 0 \end{cases} \qquad \forall x \in \left[0, L_f\right], \tag{15}$$

$$D(x) = \begin{cases} 0 & if \;\; w(x) > 0 \\ D & if \;\; w(x) \le 0 \end{cases} \qquad \forall x \in \left[0, L_f\right]. \tag{16}$$

According to Eq. (14), Eq. (15), and Eq. (16), the elastic foundation parameters are no longer constants, but they are nonlinear functions of the transverse displacement $w(x)$. As these functions are step functions where the parameters are either zero or a constant value, the simplest and most commonly used approach is to consider the stiffness matrices of the elements as either equal to the null matrix, if at least one of the nodes has a positive displacement, or equal to the expression of Eq. (11), Eq. (12), or Eq. (13), if both nodes have a negative displacement. The problem is nonlinear because, in general, the actual contact area is not known a priori, and during the solution of the system, the stiffness matrix has to be updated to account for which foundation elements are actually reacting.

If the foundation parameters also depend on x and w, Eq. (14), Eq. (15), and Eq. (16) can be modified as follows

$$k(x,w) = \begin{cases} 0 & if \;\; w(x) > 0 \\ f_k(x,w) & if \;\; w(x) \le 0 \end{cases} \qquad \forall x \in \left[0, L_f\right], \tag{17}$$

$$G_h(x,w) = \begin{cases} 0 & if \;\; w(x) > 0 \\ f_{G_h}(x,w) & if \;\; w(x) \le 0 \end{cases} \qquad \forall x \in \left[0, L_f\right], \tag{18}$$

$$D(x,w) = \begin{cases} 0 & if \;\; w(x) > 0 \\ f_D(x,w) & if \;\; w(x) \le 0 \end{cases} \qquad \forall x \in \left[0, L_f\right], \tag{19}$$

being $f_k(x,w)$, $f_{G_h}(x,w)$, and $f_D(x,w)$ general nonlinear functions of x and w.

When the foundation parameters are described by Eq. (17), Eq. (18), and Eq. (19), the foundation stiffness matrices, in general, cannot be computed analytically and are to be integrated numerically. For the numerical integration, a Gauss quadrature can be employed, and the foundation stiffness matrices can be computed as

$$\mathbf{K_{fW}} = \int_0^{L_f} k(x,w)\,\mathbf{N}^T(x)\,\mathbf{N}(x)\,dx = \\ = \sum_{i=1}^{n} \omega_i k\left(x_i, \mathbf{N}(x_i)\,\mathbf{d}\right)\mathbf{N}(x_i)^T\,\mathbf{N}(x_i), \tag{20}$$

$$\mathbf{K_{fP}} = \mathbf{K_{fW}} + \int_0^{L_f} G_h(x,w)\,\mathbf{N}^I(x)^T\mathbf{N}^I(x)\,dx = \\ = \mathbf{K_{fW}} + \sum_{i=1}^{n} \omega_i G_h\left(x_i, \mathbf{N}(x_i)\,\mathbf{d}\right)\mathbf{N}^I(x_i)^T\,\mathbf{N}^I(x_i), \tag{21}$$

$$\mathbf{K_{fH}} = \mathbf{K_{fW}} + \int_0^{L_f} D(x,w)\,\mathbf{N}^{II}(x)^T\mathbf{N}^{II}(x)\,dx = \\ = \mathbf{K_{fW}} + \sum_{i=1}^{n} \omega_i D\left(x_i, \mathbf{N}(x_i)\,\mathbf{d}\right)\mathbf{N}^{II}(x_i)^T\,\mathbf{N}^{II}(x_i), \tag{22}$$

where ω_i and x_i are the weights and the locations of the Gauss points respectively, n is the number of Gauss points, and $w(x) = \mathbf{N}(x)\,\mathbf{d}$.

Interestingly, Eq. (20), Eq. (21), and Eq. (22) are evaluated at the Gauss points of the elements and not at the nodes. This implies that, if a full integration with four Gauss points is considered, the contact condition is checked at four locations for each element instead of only at nodes. In this way, for the same mesh dimensions, a more refined definition of the contact area can be obtained. It is also worth noting, that the nodal forces computed for the elements are not the contact forces on the element, but the contact forces have to be computed back at the Gauss points during the post-processing of the results.

3.2.3. Gap implementation

For the implementation of the gap between the beam and the foundation, a nonlinear Winkler elastic foundation element with parameter $k(x, w(x))$ and an initial gap is considered. The gap is described by the function $w_0(x)$. The foundation stiffness $k(x, w(x))$ is defined as

$$k(x,w) = \begin{cases} 0 & if \ \ \Delta(x) > 0 \\ f_k(x,w) & if \ \ \Delta(x) \le 0 \end{cases} \qquad \forall x \in \left[0, L_f\right], \tag{23}$$

with $\Delta(x) = w(x) - w_0(x)$ the elongation field.

The virtual work of the Winkler element with gap can be computed for the external and internal forces respectively as

$$W_{ext} = \boldsymbol{\delta d}^T \boldsymbol{R}, \tag{24}$$

$$dW_{int} = \delta s(x)\,k(x, w(x))\,\Delta(x)\,dx, \tag{25}$$

with $\boldsymbol{\delta d}$ a vector of arbitrary node virtual displacements, $\boldsymbol{R}$ nodal forces, and $\delta s(x)$ an arbitrary virtual elongation field. The external work W_{ext} has been computed directly from the nodal variables, while the internal work dW_{int} has been computed for the infinitesimal length dx of the element. By considering

$$\delta s(x) = \boldsymbol{\delta d}^T \boldsymbol{N}^T(x), \tag{26}$$

$$w(x) = \boldsymbol{N}(x)\,\boldsymbol{d}. \tag{27}$$

Eq. (25) can be rewritten as

$$dW_{int} = \boldsymbol{\delta d}^T \boldsymbol{N}^T(x)\,k(x, w(x))\left(\boldsymbol{N}(x)\,\boldsymbol{d} - w_0(x)\right)dx. \tag{28}$$

Eq. (28) can be integrated over the length of the Winkler element as

$$W_{int} = \boldsymbol{\delta d}^T \int_0^{L_f} \boldsymbol{N}^T(x)\,k(x, w(x))\left(\boldsymbol{N}(x)\,\boldsymbol{d} - w_0(x)\right)dx. \tag{29}$$

By equating the external and internal virtual works and eliminating $\boldsymbol{\delta d}$ from both sides of the equation, through a simple algebraic manipulation, the constitutive equation of the element can be obtained

$$\boldsymbol{R} = \int_0^{L_f} \boldsymbol{N}^T(x)\,k(x, w(x))\,\boldsymbol{N}(x)\,dx\,\boldsymbol{d} \\ - \int_0^{L_f} \boldsymbol{N}^T(x)\,k(x, w(x))\,w_0(x)\,dx. \tag{30}$$

The two terms of Eq. (30) can be called as

$$\mathbf{K_{fW}} = \int_0^{L_f} \boldsymbol{N}^T(x)\,k(x, w(x))\,\boldsymbol{N}(x)\,dx, \tag{31}$$

$$\mathbf{F_{fW}} = -\int_0^{L_f} \boldsymbol{N}^T(x)\,k(x, w(x))\,w_0(x)\,dx, \tag{32}$$

being $\mathbf{K_{fW}}$ the stiffness matrix of the Winkler element already discussed in the previous sections, and $\mathbf{F_{fW}}$ the gap force vector of the Winkler element. When $\Delta(x)$ is positive, $\mathbf{F_{fW}}$ represents the forces required to balance the work of the stiffness of the elastic foundation for the gap length. Eqs. (31) and (32) are derived from the virtual work equilibrium and, thus, the force equilibrium of the solution is guaranteed and no equilibrium iteration or force adjustment coefficient is needed. Eq. (32) requires that the gap function $w_0(x)$ be integrable over the element. In case an analytical integration is not feasible, Eq. (32) can be numerically integrated by Gauss quadrature as

$$\mathbf{F_{fW}} = -\sum_{i=1}^{n} \omega_i k\left(x_i, \mathbf{N}(x_i)\,\mathbf{d}\right) w_0(x_i)\,\mathbf{N}(x_i)^T. \tag{33}$$

4. Variable reduction

In Section 3.1 the stiffness matrices of the beam elements have been derived, while in Section 3.2 the stiffness matrices of the foundation elements. In most literature papers, the two element types are assembled by constructing meshes in which the same nodes are shared by both element types (Kerr, 1964; Madhira et al., 2016; Singh and Jha, 2013; Younesian et al., 2019; Lamprea-Pineda et al., 2022), i.e. the lengths of the beam and foundation elements coincide. In Gao et al. (2015), different meshes are considered for the discretization of the beam and of the foundation. The connection between beam and foundation elements is then realized through constraint equations enforced by Lagrange multipliers. This approach has the advantage of allowing the two parts of the model to be meshed independently. However, the use of Lagrange multipliers leads to a mixed formulation, an increase in the degrees of freedom of the system, and, possibly, a more complex numerical solution of the equations.

In this paper, the different meshes used for beam and foundation are connected by a variable reduction approach. By this approach, the solving system will be a function of only the dofs of the beam elements, leading to a reduction in the system size. Additionally, no mixed formulation is required and the usual techniques for solving nonlinear systems can be employed. The variable reduction approach is also a technique suitable for implementation in a finite element code and requires only matrix multiplications.

Fig. 3 depicts a node F of a foundation element on the axis of a beam element and comprised of the two nodes B_1 and B_2 of a beam element. $\mathbf{d_{beam}} = \left[w_1 \ \ \theta_1 \ \ w_2 \ \ \theta_2\right]^T$ indicates the vector of the nodal displacements of the beam element, with w_1 and θ_1 and w_2 and θ_2 the displacements and rotations of the nodes B_1 and B_2, respectively, and $\mathbf{d_F} = \left[w_F \ \ \theta_F\right]^T$ the displacement and rotation of the node F of the elastic foundation.

As the beam deforms, node F must remain on the beam axis. Therefore, the displacement and the rotation of node F can be computed as a function of the shape functions of the beam element as

$$\begin{cases} w_F = \mathbf{N}(x_F)\,\mathbf{d_{beam}} \\ \theta_F = \mathbf{N}^I(x_F)\,\mathbf{d_{beam}} \end{cases} \Rightarrow \mathbf{d_F} = \boldsymbol{\Lambda}_F(x_F)\,\mathbf{d_{beam}}, \tag{34}$$

with $\boldsymbol{\Lambda}_F(x_F) = \begin{bmatrix} \mathbf{N}(x_F) \\ \mathbf{N}^I(x_F) \end{bmatrix}$ the Jacobian matrix defining the relationship between the dofs of node F and the displacements of the nodes of the beam element. x_F is the position of the node F on the beam element.

If a foundation element with two nodes is considered, with respect to the mesh of the beam, three different relative positions of the nodes of the foundation element and the elements of the beam mesh can occur (Fig. 4).

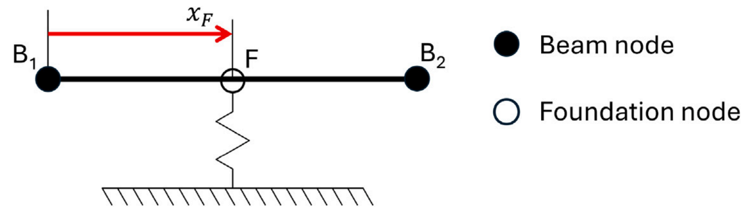

Fig. 3. Elastic foundation node F on the axis of a beam element with nodes B_1 and B_2. x_F is the position of the node F on the beam axis in the beam reference system.

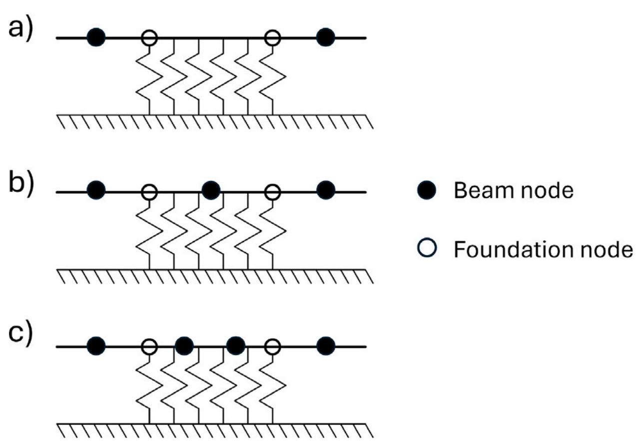

Fig. 4. Relative positioning of the nodes of the foundation element and the nodes of the mesh of the beam.

(a) Both nodes of the foundation element belong to the same beam element (Fig. 4a). In this case, if the same shape functions are used for both the beam and for foundation element, the foundation element undergoes the same deformation of the beam element at every point. The limit situation of this case occurs when the nodes of the foundation element and of the beam element coincide. This situation corresponds to using the same mesh for both the beam and the foundation, and it can be formally addressed using the proposed approach.

(b) One node of the foundation element belongs to one element of the beam and the other to a neighbouring element of the beam (Fig. 4b). In this case, the foundation element undergoes a different deformation than the corresponding beam elements. However, if the foundation element is sufficiently smaller, such a difference is small. When its dimension is vanishing, the deformation of the foundation element tends to the deformation of the beam elements .

(c) One node of the foundation element belongs to one element of the beam and the other to a non-neighbouring element of the beam (Fig. 4c). In this case, the foundation element undergoes a different deformation than the corresponding beam elements and the size of the foundation element cannot be reduced to reduce this difference.

Case a is the best case and, if the same shape functions are adopted for the two element types, no discretization error is introduced between the two meshes. If different shape functions are used, the displacements of the foundation element tend to the displacements of the beam element as the dimension of the foundation element is reduced. However, to ensure that any foundation element belongs to this case, all of the nodes of the beam must be also used as nodes in the foundation mesh. In other words, the foundation mesh can have more elements than the beam mesh but must contain all nodes of the latter. To avoid this constraint, some discretization error has to be accepted. For elements belonging to case b, the discretization error can be reduced by reducing the size of the foundation elements, and, at the limit, the process is convergent. Therefore, case b is acceptable. In this case, a convergence analysis can be used to define the appropriate mesh dimensions. Conversely, case c must be avoided as, in this case, the discretization error cannot be controlled. As a consequence, to apply this method with acceptable discretization errors, the elements of the foundation mesh have to be smaller than the elements of the beam mesh. Therefore, the number of foundation elements must be greater than, or at most equal to, the number of beam elements.

If a Winkler element with gap is considered, the variable reduction approach can be applied as follows. By considering Eq. (34), the Jacobian matrix between the displacements of the nodes of the foundation element ($\mathbf{d}_1$ and $\mathbf{d}_2$) and the displacements of all the nodes of the beam mesh ($\mathbf{d_{beam}}$) can be defined as

$$\begin{cases} \mathbf{d}_1 = \boldsymbol{\Lambda}_{d1}\left(x_{\mathbf{d}_1}\right)\mathbf{d_{beam}} \\ \mathbf{d}_2 = \boldsymbol{\Lambda}_{d2}\left(x_{\mathbf{d}_2}\right)\mathbf{d_{beam}} \end{cases} \Rightarrow \mathbf{d} = \boldsymbol{\Lambda}\mathbf{d_{beam}}, \tag{35}$$

where $\mathbf{d} = \begin{bmatrix} \mathbf{d}_1 \\ \mathbf{d}_2 \end{bmatrix}$, and $\boldsymbol{\Lambda}$ is the global Jacobian matrix obtained by assembling $\boldsymbol{\Lambda}_{d1}$ and $\boldsymbol{\Lambda}_{d2}$, with $\boldsymbol{\Lambda}_{d1}$ and $\boldsymbol{\Lambda}_{d2}$ being the two Jacobian matrices of the nodes of the foundation element with respect to the beam element corresponding to each node and defined in Eq. (34). $x_{\mathbf{d}_1}$ and $x_{\mathbf{d}_2}$ are the coordinates of the nodes of the foundation element on the corresponding beam elements. It is worth noting that Eq. (35) remains consistent regardless of the relative positions of the two nodes of the foundation element and the elements of the beam mesh. The two Jacobian matrices, $\boldsymbol{\Lambda}_{d1}$ and $\boldsymbol{\Lambda}_{d2}$, are calculated separately for each node of the foundation element and then assembled into the global Jacobian matrix $\boldsymbol{\Lambda}$. This assembly is done with respect to the vector of all nodal displacements of the beam, $\mathbf{d_{beam}}$, at the positions corresponding to the involved nodes of the beam mesh, following the standard assembly rules of the finite element method.

By considering Eq. (35), Eq. (24) and (29) can be rewritten as

$$W_{ext} = \left(\boldsymbol{\Lambda}\delta\boldsymbol{d}_{\boldsymbol{beam}}\right)^T \boldsymbol{R}, \tag{36}$$

$$W_{int} = \left(\boldsymbol{\Lambda}\delta\boldsymbol{d}_{\boldsymbol{beam}}\right)^T \int_0^{L_f} \boldsymbol{N}^T(x)\, k\left(x, w(x)\right)\left(\boldsymbol{N}(x)\left(\boldsymbol{\Lambda}\boldsymbol{d}_{\boldsymbol{beam}}\right) - w_0(x)\right) dx, \tag{37}$$

where the integrals are performed on the coordinate of the foundation element and $\mathbf{N}(x)$ are its shape functions. As $\boldsymbol{\Lambda}$ and $\boldsymbol{d}_{\boldsymbol{beam}}$ do not depend on the x coordinate of the foundation element, by following the same computations of Section 3.2.3, the following relationships can be obtained.

$$\mathbf{K_{fW,beam}} = \boldsymbol{\Lambda}^T \int_0^{L_f} \boldsymbol{N}^T(x)\, k\left(x, w(x)\right) \boldsymbol{N}(x)\, dx \boldsymbol{\Lambda} = \boldsymbol{\Lambda}^T \mathbf{K_{fW}} \boldsymbol{\Lambda}, \tag{38}$$

$$\mathbf{F_{fW,beam}} = -\boldsymbol{\Lambda}^T \int_0^{L_f} \boldsymbol{N}^T(x)\, k\left(x, w(x)\right) w_0(x)\, dx = \boldsymbol{\Lambda}^T \mathbf{F_{fW}}. \tag{39}$$

$\mathbf{K_{fW}}$ and $\mathbf{F_{fW}}$ are the stiffness matrix and the gap force vector computed in the foundation element reference system, while $\mathbf{K_{fW,beam}}$ and $\mathbf{F_{fW,beam}}$ are the stiffness matrix and the gap force vector referenced to the beam mesh. These last two terms can be assembled with the stiffness matrix and the load vector of the beam, respectively.

Similarly, the stiffness matrices of the Pasternak and Hetényi foundation elements can be expressed as

$$\mathbf{K}_{\mathbf{fp,beam}} = \boldsymbol{\Lambda}^T \mathbf{K}_{\mathbf{fp}} \boldsymbol{\Lambda}, \tag{40}$$

$$\mathbf{K}_{\mathbf{fh,beam}} = \boldsymbol{\Lambda}^T \mathbf{K}_{\mathbf{fh}} \boldsymbol{\Lambda}. \tag{41}$$

The resulting solving system, without gap, assumes the form

$$\left(\mathbf{K}_{\mathbf{i}} + \mathbf{K}_{\mathbf{fj,beam}}\right) \boldsymbol{d}_{\boldsymbol{beam}} = \mathbf{F}, \tag{42}$$

where $\mathbf{K}_{\mathbf{i}}$ $(i = B, T, G)$ is the beam stiffness matrix, defined according to the different beam models. $\mathbf{K}_{\mathbf{fj,beam}}$ $(j = w, p, h)$ is the foundation stiffness matrix referred to the beam mesh nodes defined according to the different foundation formulations. $\mathbf{F}$ is the vector of the nodal forces applied to the beam.

For the Winkler foundation with gap, the solving system can be expressed as

$$\left(\mathbf{K}_{\mathbf{i}} + \mathbf{K}_{\mathbf{fW,beam}}\right) \boldsymbol{d}_{\boldsymbol{beam}} = \mathbf{F} + \mathbf{F}_{\mathbf{fW,beam}}, \tag{43}$$

being $\mathbf{F}_{\mathbf{fW,beam}}$ the gap force vector of the Winkler foundation referred to the beam mesh nodes.

The systems of Eqs. (42) and (43) are functions of the sole dofs of the nodes of the beam. The mesh of the elastic foundation can be refined without increasing the dimension or the complexity of the solving systems. The displacements of the nodes of the elastic foundation can be computed from the displacements of the nodes of the beam by using Eq. (35) in the post-processing phase.

All the terms of Eq. (42) could be functions of the nodal displacements, therefore, in general, the system is nonlinear. The system of Eq. (43) is always nonlinear as a gap function is considered. The solution of a nonlinear FE problem is widely discussed in the literature and it is outside the scope of this paper. The solutions of Eq. (42) and (43) can be obtained by the usual methods employed to solve such problems. In the following numerical examples, a simple direct substitution method is used. The direct substitution method, also known as fixed-point iteration, involves computing the updated values of the unknown variables as a function of their values at the previous iteration and repeating the iterations to refine the solution until it stabilizes below some desired tolerance or the maximum number of iterations is reached (Chapra and Canale, 2009). The method is iterative and can be used to solve most numerical problems, even if it is characterized by a relatively slow convergence rate and, in some cases, convergence issues.

5. Numerical examples

In this section, three numerical examples are considered. The first two examples are taken from Gao et al. (2015) and Froio and Rizzi (2016), respectively, and are used to validate the method developed in this paper. The third example presents a highly nonlinear elastic foundation with a gap. All the following examples are solved by considering the numerical formulation of the foundation elements reported in Section 3.2.2 and Section 3.2.3, with four Gauss points for each element.

5.1. Example 1: linear unilateral foundation with different beam elements

In Fig. 5 top the first example is depicted. This example has been taken from Gao et al. (2015) and the positive direction of the displacement w has been directed downward to be consistent with the reference. Also, to allow for the validation of the method presented in this paper with already published results, the same mesh, structure configuration, and data reported in Gao et al. (2015) are used.

The example consists in a beam with three supports on a linear unilateral elastic foundation without gap. The supports are at the extremities and at the centre of the beam. Three forces are applied to the beam, namely $F_1 = 10^7$ N, $F_2 = -510^6$ N, and $F_3 = 510^7$ N. The beam has a length of 4000 mm and the three forces are applied at 1000 mm, 3000 m, and 4000 mm from the left end, respectively. The beam has a rectangular cross-section with height of 200 mm and width of 1000 mm. The material is linear with a Young modulus of 30 000 MPa and a Poisson's ratio of 0.3. The elastic foundation has a constant stiffness of 20 N/mm^2. The example is solved twice, once with an Euler–Bernoulli beam formulation and once with a Gao beam formulation. The beam displacements and the elastic foundation reaction forces, computed for the two beam formulations considering eight beam elements and sixteen foundation elements, are reported in Fig. 5 bottom.

Table 1 and Table 2 report the displacements computed for the Euler–Bernoulli and Gao beam formulations respectively. The tables also show the comparison between the displacements computed in Gao et al. (2015) and by using the method presented in this paper. The two methods are in very good agreement. The method presented in Gao et al. (2015) shows slower convergence with the number of foundation elements because it employs different element formulations for the foundation and the beam, while the method presented in this paper uses the same element formulation for both meshes.

Referring to the convergence of the method presented in this paper, by inspecting Table 1 and Table 2, it can be observed that the results do not change as the number of foundation elements increases. This is due to two reasons. First, the meshes used to solve the examples have been taken from Gao et al. (2015), and in all cases, all nodes of the foundation elements correspond to nodes of the beam mesh. In this case, no discretization error is present when the same shape functions are used for the two meshes. Second, the contact area is delimited by the node at 2000 mm, as at that point a constraint is present. For all the considered foundation element meshes, a node of these meshes is also present in that location. Therefore, in all cases, the contact area is defined without any discretization error. The convergence of the presented method will be discussed in the example in Section 5.3.

5.2. Example 2: foundation with spatially varying stiffness

In this example, a published analytical solution of a beam on an elastic foundation is used as a benchmark for the method presented in this paper. Several examples of analytical solutions of beams on elastic foundations can be found in the literature (Franklin and Scott, 1979; Liang et al., 2014; Froio and Rizzi, 2016, 2017). Among the available cases, the simply supported beam loaded with a constant distributed load q on an elastic foundation with spatially varying stiffness discussed in Froio and Rizzi (2016) is considered. The example is depicted in Fig. 6 left. The stiffness spatial variation is described by

$$k(x) = \frac{1}{\left(c_0 + c_1 x\right)^4}, \tag{44}$$

with $c_0 > 0$ and $c_1 > -\frac{c_0}{L}$. In Froio and Rizzi (2016), for the analytical formulation of the solution, the partial derivative equation describing the system is given as function of functional terms as

$$(1+\beta\xi)^4 \, v^{IV}(\xi) + \frac{v(\xi)}{\alpha^4} = \frac{qL^4}{EJ}(1+\beta\xi)^4, \tag{45}$$

where $\xi = \frac{x}{L}$, $\beta = \frac{c_1 L}{c_0}$, and $\alpha = \sqrt[4]{EJ}\,\frac{c_0}{L}$. By using these functionals and reporting the results in normalized form with respect to the maximum deflection, the solution becomes independent of the beam length L, the elastic modulus of the material E, the moment of inertia of the beam cross-section J, and from the value of the applied load q. In the following, the case with $\alpha = 0.177$ and $\beta = -0.9$ is considered, as it is the same case considered in Froio and Rizzi (2016) for the validation of the analytical solution to the problem. Fig. 6 right depicts the corresponding spatial variation of the foundation stiffness. A logarithmic scale has been applied to the y-axis to better illustrate the variation across different orders of magnitude.

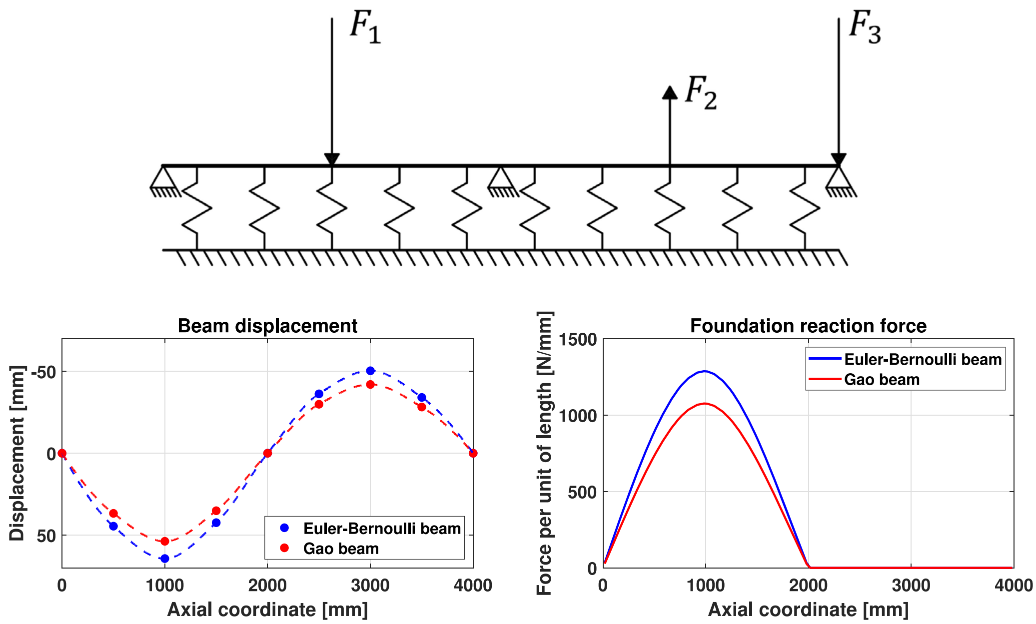

Fig. 5. Top: sketch of Example 1, adapted from Gao et al. (2015). Bottom: beam deformation and foundation reaction forces per unit of length obtained by the method presented in this paper with eight beam elements and sixteen foundation elements.

Table 1
Comparison of the maximum and minimum computed displacement between the presented method and the approach described in Gao et al. (2015), Bernoulli beam elements.

Bernoulli beam with 4 elements

	Results in Gao et al. (2015)		Presented method results	
# foundation elements	*w max* [mm]	*w min* [mm]	*w max* [mm]	*w min* [mm]
16	64.40	−50.39	64.31	−50.35
40	64.33	−50.36	64.31	−50.35
80	64.32	−50.35	64.31	−50.35

Bernoulli beam with 8 elements

	Results in Gao et al. (2015)		Presented method results	
# foundation elements	*w max* [mm]	*w min* [mm]	*w max* [mm]	*w min* [mm]
16	64.40	−50.39	64.32	−50.35
40	64.33	−50.36	64.32	−50.35
80	64.32	−50.36	64.32	−50.35

Table 2
Comparison of the maximum and minimum computed displacement between the presented method and the approach described in Gao et al. (2015), Gao beam elements.

Gao beam with 4 elements

	Results in Gao et al. (2015)		Presented method results	
# foundation elements	*w max* [mm]	*w min* [mm]	*w max* [mm]	*w min* [mm]
16	53.68	−41.93	53.63	−41.91
40	53.64	−41.91	53.63	−41.91
80	53.64	−41.91	53.63	−41.91

Gao beam with 8 elements

	Results in Gao et al. (2015)		Presented method results	
# foundation elements	*w max* [mm]	*w min* [mm]	*w max* [mm]	*w min* [mm]
16	53.81	−42.00	53.76	−41.99
40	53.77	−41.99	53.76	−41.99
80	53.77	−41.99	53.76	−41.99

Fig. 7 left reports the comparison between the displacement computed by the analytical solution derived in Froio and Rizzi (2016) and the nodal displacements computed by the method presented in this paper. The expression of the analytical solution is rather complicated and it is not provided in this paper. Interested readers can refer to Froio and Rizzi (2016). For the numerical solution, ten Euler–Bernoulli elements of equal length have been used for the discretization

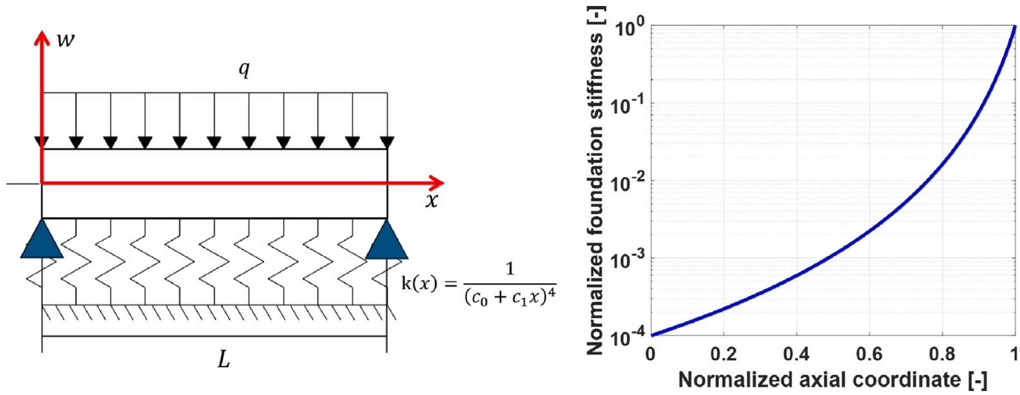

Fig. 6. Beam on a foundation with spatially varying stiffness. Left: scheme of the structure. Right: stiffness variation as function of the normalized axial coordinate $\xi = \frac{x}{L}$ for $\alpha = 0.177$ and $\beta = -0.9$ (see Eq. (45)).

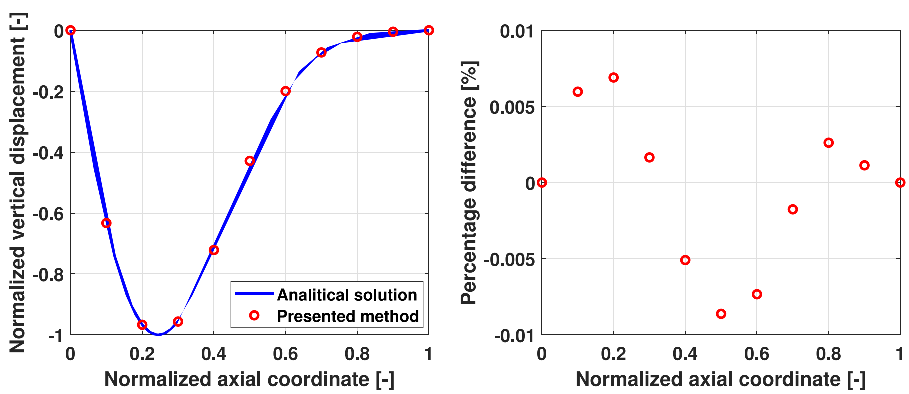

Fig. 7. Comparison of the displacements computed for a beam on an elastic foundation with spatially varying stiffness with the analytical solution in Froio and Rizzi (2016) and with the method presented in this paper. Left: displacements normalized with respect to the maximum deflection. Right: percentage displacement difference.

of the beam, while thirty-four elements of equal length have been considered for the foundation. This discretization ensures that only the first and last nodes are shared by the two meshes. In Fig. 7 right, the percentage difference between the computed displacements is reported. The agreement between the two solutions is very good with a maximum difference below 0.01%. As a comparison, in Froio and Rizzi (2016) the analytical solution is compared with three different numerical methods for the solution of differential equations, namely the finite power series (Clastornik et al., 1986), the sine series expansion (Iyengar and Anantharamu, 1963), and the central-difference scheme (Bowles, 1974). With a comparable number of nodes with respect to the mesh used in Fig. 7, the maximum differences between these three numerical methods and the analytical solution is between 1% and 15%.

5.3. Example 3: nonlinear foundation with gap

Fig. 8 illustrates the third example. The example could be considered a simplified model of a pipe on a terrain. The beam, of hollow circular cross-section, is subjected to a uniform load, corresponding to the weight of the pipe, and rests on a nonlinear foundation with a gap representing the terrain. Slider constraints are applied at both ends of the beam to model the remainder of the pipe. The foundation has a complex shape. From the left slider to point A, there is no gap between the beam and the foundation. At point A, the foundation has a vertical drop and, from that point, a gap is present. Finally, between points B and C, a sinusoidal shape is considered for the gap.

The stiffness of the foundation spring is nonlinear and described by the expression

$$k = n k_0 \Delta z^{n-1}, \tag{46}$$

Table 3
Parameters of the example of Fig. 8.

Parameter	Value
Beam length	50 m
Beam cross-section external diameter	0.4 m
Beam cross-section internal diameter	0.3 m
Beam material elastic modulus	10^7 N/m^2
Beam material Poisson coefficient	0.3
Distributed load q	2500 N/m
x coordinate of point A	20 m
x coordinate of point B	38 m
x coordinate of point C	44 m
Gap mean height h	0.5 m
Amplitude of the gap sinusoid h_A	0.2 m
Foundation parameter k_0	60 000 N/m^2
Foundation parameter n	2

which can represent a simplified relationship between sinkage Δz and terrain stiffness (Bekker, 1969). The sinkage Δz represents the deformation of the foundation. k_0 and n represent the terrain properties taking into account the dimensions of the body on the terrain. In particular, n defines the nonlinearity of the stiffness characteristics. If $n > 1$ the stiffness is hardening, otherwise is softening. As hardening problems are more critical from a numerical point of view, in this example, the case $n > 1$ is considered. Hardening problems are typical of most contact situations. The data of the problem is summarized in Table 3. The problem is solved using Euler–Bernoulli beam elements and a Winkler foundation.

Fig. 9 depicts the displacements computed for the beam by using 25 Euler–Bernoulli beam elements and 100 Winkler foundation elements.

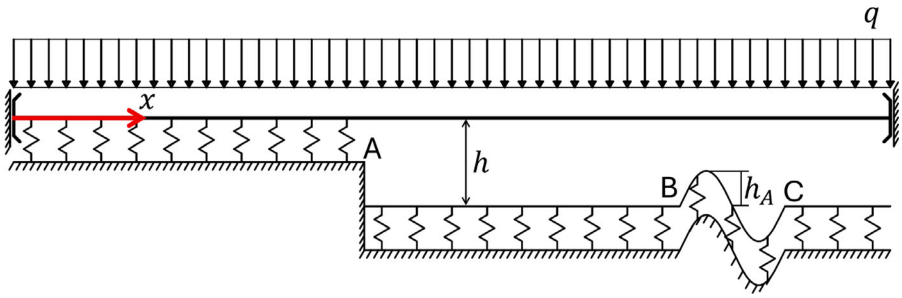

Fig. 8. Sketch of Example 3.

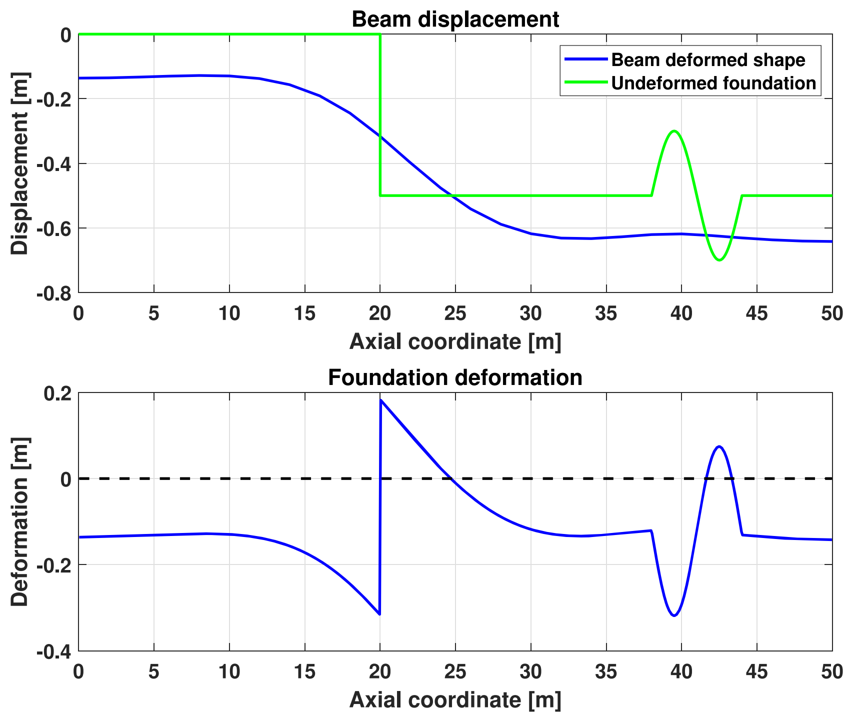

Fig. 9. Displacements of the beam of Example 2 depicted in Fig. 8 (data in Table 3). Solution obtained with 25 Bernoulli beam elements and 100 Winkler foundation elements. Top: beam displacements. Bottom: foundation deformation.

At the top, the deformed shape of the beam is compared with the undeformed foundation. At the bottom, the deformation of the foundation elements is shown. Negative deformation indicates contact between the beam and the foundation. From the left slider to point A, the beam remains in contact with the foundation. After point A, as a discontinuity is present in the foundation with a quite large gap, the beam and the foundation are not in contact up to where the displacement of the beam is sufficient to close the gap. The first section of the sinusoidal part of the foundation causes a reduction in the deformation of the beam as the initial gap is smaller. Then, in the second section, the increase in the initial gap is quite sharp and the beam loses contact with the foundation. The contact areas are not known a priori, but are computed during the solution of the system. The computed total length of the contact area is 43.6 m.

The stiffness per unit of length of the foundation computed at each Gauss point of the foundation elements is reported in Fig. 10 top. As the stiffness is nonlinear, at any point of the foundation a different value of stiffness is computed accordingly to Eq. (46) and to the beam displacement. Where the beam is not in contact with the foundation, a null stiffness is considered. In Fig. 10 middle, the reaction force of the foundation is depicted. The reaction force is computed in the post-processing phase, after the foundation stiffness and deformation have been determined. Fig. 10 bottom shows the values of the gap forces. These forces are computed at each Gauss point, integrated as shown in Eq. (33), and then added to the known force vector (see Eqs. (39) and (42)), for the computation of the beam displacement. The gap forces are null where the gap is null or where there is no contact between the beam and the foundation. Between points A and B, even if the gap is constant (see Fig. 8), the gap force is not, since the stiffness is not constant in this region. The same happens between point C and the right slider.

The convergence analysis of the solution of this example is reported in Fig. 12 and Table 4, Table 5, and Table 6. The convergence analysis have been performed by always using 25 equally spaced Euler–Bernoulli beam elements for the beam and varying the number of foundation elements. In the analysis, displacement, foundation stiffness, and foundation reaction force at point A are considered. This point has been selected due to the presence of a gap discontinuity at this location.

For the convergence analysis, three different strategies have been considered for refining the foundation mesh. The three strategies are depicted in Fig. 11 and are as follows.

(a) *Corresponding nodes* (Fig. 11a): each node of the beam mesh has a corresponding node on the foundation mesh. In this case, each element of the foundation mesh is fully contained within a single

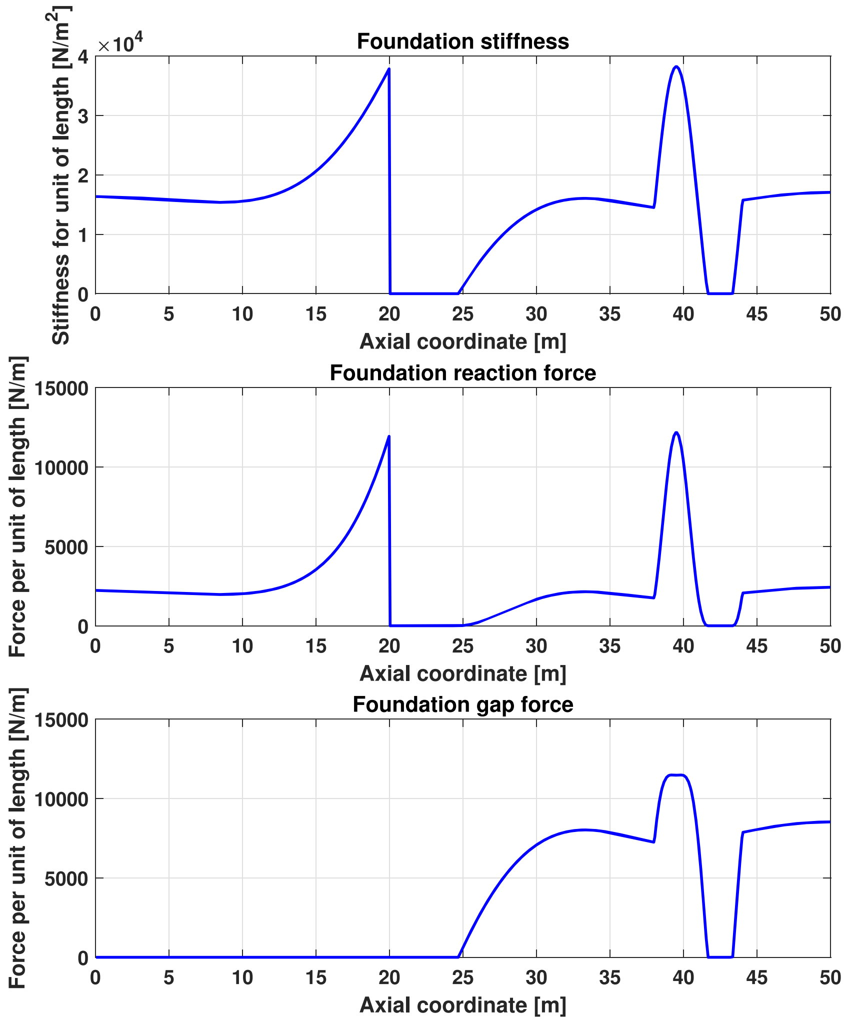

Fig. 10. Foundation stiffness and reaction forces of Example 2 depicted in Fig. 8 (data in Table 3). Solution obtained with 25 Bernoulli beam elements and 100 Winkler foundation elements. Top: foundation stiffness per unit of length. Middle: foundation reaction force per unit of length. Bottom: foundation gap forces for unit of length.

element of the beam mesh, matching the relative positioning of the beam and foundation elements depicted in Fig. 4a. As explained in Section 4, no discretization error is expected for this mesh configuration.

(b) Non-corresponding nodes (Fig. 11b): There is no correspondence between the nodes of the beam and foundation meshes. In this case, some elements of the foundation mesh are not fully contained within a single element of the beam mesh but instead span two adjacent beam elements. These elements have a relative node positioning similar to the situation depicted in Fig. 4b. As explained in Section 4, a discretization error is expected for these nodes. This error should diminish as the foundation mesh is refined.

(c) *Local refinement* (Fig. 11c): the foundation mesh is locally refined. For the considered example, mesh refinement is applied within a region of ± 0.1 m around point A. Outside the mesh refinement region, 24 equally spaced Winkler foundation elements have been used for any increase in the local refinement. Since there is no correspondence between the nodes of the refined mesh and the nodes of the beam, a discretization error is present.

For all the quantities reported in Fig. 12, the approach developed in this paper shows a different convergence behaviour for the mesh refinement strategies shown in Fig. 11a *Corresponding nodes* and Fig. 11b *Non-corresponding nodes*. In particular, convergence in the first case is faster, especially in terms of displacements. This difference arises because discretization errors occur only when some elements of the foundation mesh span two adjacent elements of the beam mesh. Since this error is absent in the *Corresponding nodes*, as expected, a faster convergence rate is achieved. However, as the foundation mesh size is reduced, the error for the case in which the discretization error is present, namely case *Non-corresponding nodes* (Fig. 11b), also reduces

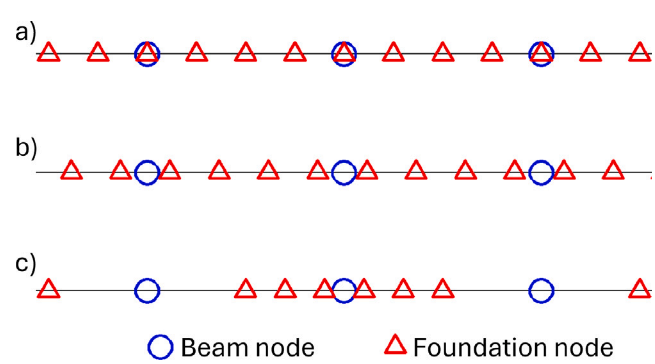

Fig. 11. Meshes for the convergence analysis of Example 3. (a) *Corresponding nodes*: any node of the beam mesh has a corresponding node on the foundation mesh. (b) *Non-corresponding nodes*: there is no correspondence between the nodes of the beam and foundation meshes. (c) *Local refinement*: the foundation mesh is locally refined.

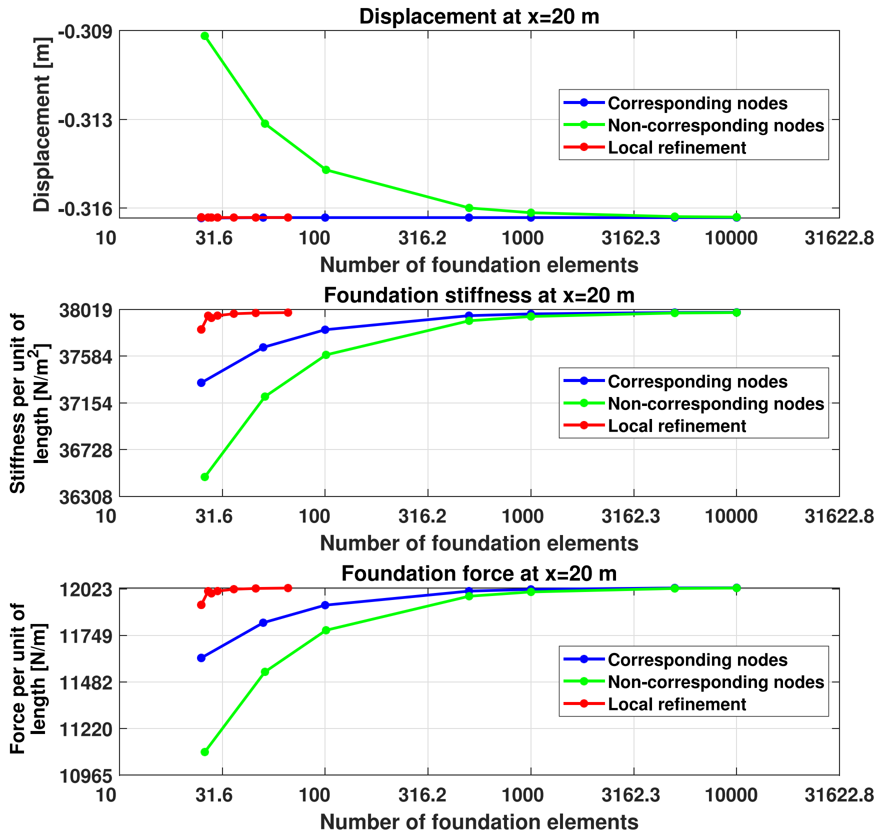

Fig. 12. Convergence of the solution of Example 3 as function of the number of Winkler foundation elements (data in Table 3). For any number of foundation elements, 25 equally spaced Euler–Bernoulli elements have been used for the beam. The convergence is evaluated at $x = 20$ m as in this point a discontinuity in the foundation geometry is present. Plots in bilogarithmic scale. Top: displacement. Centre: foundation stiffness force per unit of length. Bottom: foundation reaction force for unit of length.

Table 4
Convergence analysis of the Example 3 as function of the number of Winkler foundation elements (data in Table 3, 25 beam elements). The nodes of the foundation mesh are equally spaced. All nodes of the beam mesh also belong to the foundation mesh.

# foundation elements	w [m]	k [N/m^2]	Reaction force [N]	Found. elem. size [m]
25	−0.31661	37 339	11 618	2
50	−0.31662	37 666	11 823	1
100	−0.31662	37 830	11 926	0.5
500	−0.31662	37 961	12 009	0.1
1000	−0.31662	37 978	12 019	0.05
5000	−0.31662	37 991	12 027	0.01
10 000	−0.31662	37 992	12 029	0.005

Table 5
Convergence analysis of the Example 3 as function of the number of Winkler foundation elements (data in Table 3, 25 beam elements). The nodes of the foundation mesh are equally spaced. The nodes of the beam mesh do not belong to the foundation mesh.

# foundation elements	w [m]	k [N/m^2]	Reaction force [N]	Found. elem. size [m]
26	−0.30924	36 482	11 091	1.92
51	−0.31278	37 212	11 539	0.980
101	−0.31466	37 596	11 779	0.495
501	−0.3622	37 913	11 978	0.0998
1001	−0.31642	37 954	12 004	0.04995
5001	−0.31658	37 986	12 024	0.009998
10 001	−0.31660	37 990	12 027	0.0049995

and the solution converges to the same solution of the first case, namely *Corresponding nodes* (Fig. 11a).

In the two described cases, the nodes of the foundation meshes are equally spaced. When local mesh refinement is applied around point A (Fig. 11c, *Local refinement*), a large increase in the convergence rate can be observed, as shown in Fig. 12. This analysis shows that refining the foundation mesh in the discontinuity region yields better results than uniformly refining the foundation mesh. When 66 foundation elements are used, results are obtained that closely match those from using 5000 foundation elements in the *Corresponding nodes* case or 10 000 foundation elements in the *Non-corresponding nodes* case.

Fig. 13 shows the computational times for a single iteration of the iterative solution algorithm for the refined meshes considered in Table 4. The computational time increases linearly with the number of foundation mesh elements. This is consistent with the proposed algorithm. In fact, as the number of foundation mesh elements increases, the time for constructing the foundation mesh also increases proportionally. The time required for the solution of the solving system (Eq. (43)) remains unchanged, as depends only on the number of nodes in the beam mesh. In fact, the only free variables of the system are the displacements of the nodes of the beam mesh.

Table 6
Convergence analysis of the Example 3 as function of the number of Winkler foundation elements (data in Table 3, 25 beam elements). Foundation mesh refinement. The nodes of the beam mesh do not belong to the foundation mesh.

# foundation elements	w [m]	k [N/m^2]	Reaction force [N]	Min. found. elem. size [m]
25	−0.31661	37 832	11 927	0.2
27	−0.31661	37 961	12 009	0.1
28	−0.31661	37 940	11 995	0.067
30	−0.31661	37 962	12 009	0.04
36	−0.31661	37 979	12 020	0.0182
46	−0.31661	37 986	12 024	0.0095
66	−0.31661	37 990	12 027	0.00488

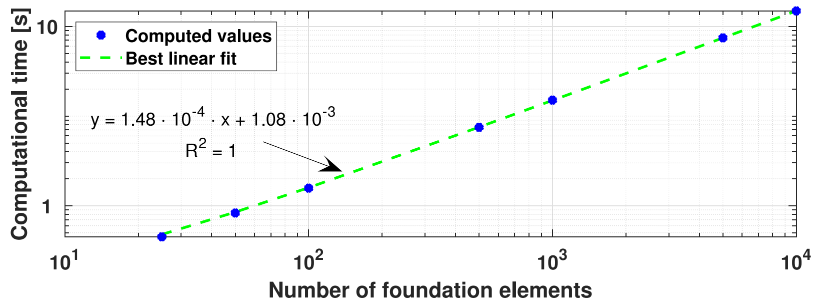

Fig. 13. Computational time for the different refined foundation meshes of Example 3 reported in Table 4. The computational time refers to one iteration of the solution on a Intel I7-12700H laptop processor, code not optimized for speed.

6. Conclusions

In this paper, the finite element modelling of a beam resting on an elastic foundation has been discussed. A general method to decouple the meshes of the beam and of the foundation has been presented. The method consists of independently meshing the beam and the foundation. Then, the nodes of the foundation mesh are constrained to remain on the axis of the beam through geometrical constraints enforced by a variable reduction approach.

Although the concept of decoupling the two meshes is not new, the presented method is much simpler than other methods presented in the literature, offering several advantages.

The method is based on the variable reduction approach, a well-known technique and can be formalized in the finite element formulation. This approach avoids increasing the dimension of the solving system when finer meshes are used to describe the elastic foundation. Furthermore, it does not require special solution techniques, as standard finite element solution methods can be employed.

The method is quite general, as it can be applied to any formulation of the beam and foundation elements. Even different shape functions can be used for the two kinds of elements. Both linear and nonlinear beam and elastic foundation element formulations can be employed. The application of the method for some beam and elastic foundation formulations has been shown.

The formulation of the method allows for a straightforward inclusion of a gap between the beam and the elastic foundation. A suitable gap formulation has been developed for the Winkler elastic foundation model along with the implementation in the finite element framework. The general applicability of the presented method has been shown for this case as well.

The paper shows that the only constraint in the application of the method is that the elements of the foundation have to be smaller than, or at least equal in size to, the elements of the beam. This is not a limitation, as the scope of using different meshes is to allow for the refinement of the foundation mesh. In this respect, local mesh refinement can be used effectively, especially in cases with discontinuities in foundation characteristics.

Three examples have been considered to demonstrate the performances of the method. The first two examples are taken from the literature and serve as benchmarks for evaluating the accuracy of the developed method against existing results. The results show that the method is able to accurately solve these problems, even when a nonlinear beam formulation is used.

The third example involves a nonlinear elastic foundation with an initial gap of variable width relative to the beam. The gap is present only in part of the beam, and a geometrical discontinuity occurs where the gap begins. The method has proven effective in solving the problem and identifying the contact areas. The example has also been used to illustrate the convergence of the method as a function of the dimensions of the foundation elements for a given beam mesh. The analysis shows that better results are obtained when each foundation element is fully contained within a single beam element, as opposite to when some foundation elements span two adjacent beam element. This effect is due to the discretization error in the foundation mesh, which occurs only in the latter case. However, as the foundation mesh is reduced, the discretization error reduces as well and the solution of the two cases converges to the same values. Finally, if a local refinement is applied in the gap's discontinuity zone, very accurate results can be obtained with a significantly smaller number of foundation elements.

The presented method has been discussed in a two-dimensional framework. Further development could involve extending the method to three-dimensional problems and including the axial deformation of the beam.

CRediT authorship contribution statement

Giorgio Previati: Writing – review & editing, Writing – original draft, Supervision, Resources, Project administration, Methodology, Investigation, Formal analysis, Conceptualization. **Federico Ballo:** Writing – review & editing, Writing – original draft, Visualization, Validation, Software, Methodology, Investigation, Formal analysis, Data curation. **Pietro Stabile:** Writing – original draft, Visualization, Validation, Software, Investigation, Formal analysis, Data curation.

Declaration of competing interest

The authors declare that they have no known competing financial interests or personal relationships that could have appeared to influence the work reported in this paper.

Appendix A. Euler–Bernoulli and Timoshenko beams stiffness matrices

Euler–Bernoulli beam stiffness matrix (see Fig. 2 for symbols' definition):

$$\mathbf{K_B} = \frac{EI}{L}\begin{bmatrix} \frac{12}{L^2} & \frac{6}{L} & -\frac{12}{L^2} & \frac{6}{L} \\ \frac{6}{L} & 4 & -\frac{6}{L} & 2 \\ -\frac{12}{L^2} & -\frac{6}{L} & \frac{12}{L^2} & -\frac{6}{L} \\ \frac{6}{L} & 2 & -\frac{6}{L} & 4 \end{bmatrix}. \tag{A.1}$$

Timoshenko beam stiffness matrix:

$$\mathbf{K_T} = \frac{EI}{L\,(\phi+1)}\begin{bmatrix} \frac{12}{L^2} & \frac{6}{L} & -\frac{12}{L^2} & \frac{6}{L} \\ \frac{6}{L} & \phi+4 & -\frac{6}{L} & 2-\phi \\ -\frac{12}{L^2} & -\frac{6}{L} & \frac{12}{L^2} & -\frac{6}{L} \\ \frac{6}{L} & 2-\phi & -\frac{6}{L} & \phi+4 \end{bmatrix}, \tag{A.2}$$

where $\phi = \frac{12EI}{\kappa GAL^2}$ and the following shape functions have been considered to take into account the shear deformation

$$\mathbf{N}_{\phi} = \frac{1}{1+\phi}\begin{bmatrix} \frac{2x^3}{L^3} - \frac{3x^2}{L^2} + 1 + \left(1 + \frac{x}{L}\right)\phi \\ x - \frac{2x^2}{L} + \frac{x^3}{L^2} + \left(\frac{x}{2} - \frac{x^2}{2L}\right)\phi \\ \frac{3x^2}{L^2} - \frac{2x^3}{L^3} + \frac{x}{L}\phi \\ \frac{x^3}{L^2} - \frac{x^2}{L} - \left(\frac{x}{2} - \frac{x^2}{2L}\right)\phi \end{bmatrix}^T. \tag{A.3}$$

Appendix B. Non linear term of the Gao beam stiffness matrix

By considering Eq. (A.1), the stiffness matrix of the Gao beam element reads (see Fig. 2 for symbols' definition)

$$\mathbf{K_G} = \mathbf{K_B} + \frac{E\alpha}{3}\begin{bmatrix} k_{G,11} & k_{G,12} & k_{G,13} & k_{G,14} \\ k_{G,12} & k_{G,22} & k_{G,23} & k_{G,24} \\ k_{G,13} & k_{G,23} & k_{G,33} & k_{G,34} \\ k_{G,14} & k_{G,24} & k_{G,34} & k_{G,44} \end{bmatrix}, \tag{B.1}$$

where:

$$k_{G,11} = \left(L\left(\frac{18\,\theta_1\,w_1}{35} - \frac{18\,\theta_1\,w_2}{35} + \frac{18\,\theta_2\,w_1}{35} - \frac{18\,\theta_2\,w_2}{35}\right) - \frac{144\,w_1\,w_2}{35} + L^2\left(\frac{3\,{\theta_1}^2}{35} + \frac{3\,{\theta_2}^2}{35}\right) + \frac{72\,{w_1}^2}{35} + \frac{72\,{w_2}^2}{35}\right)/L^3, \tag{B.2}$$

$$k_{G,12} = \frac{\theta_1\,\theta_2}{70} + \frac{L\left(\frac{6\,\theta_1\,w_1}{35} - \frac{6\,\theta_1\,w_2}{35}\right) - \frac{18\,w_1\,w_2}{35} + \frac{9\,{w_1}^2}{35} + \frac{9\,{w_2}^2}{35}}{L^2} - \frac{{\theta_1}^2}{140} + \frac{{\theta_2}^2}{140}, \tag{B.3}$$

$$k_{G,13} = \left(-L\left(\frac{18\,\theta_1\,w_1}{35} - \frac{18\,\theta_1\,w_2}{35} + \frac{18\,\theta_2\,w_1}{35} - \frac{18\,\theta_2\,w_2}{35}\right) - \frac{144\,w_1\,w_2}{35} + L^2\left(\frac{3\,{\theta_1}^2}{35} + \frac{3\,{\theta_2}^2}{35}\right) + \frac{72\,{w_1}^2}{35} + \frac{72\,{w_2}^2}{35}\right)/L^3, \tag{B.4}$$

$$k_{G,14} = \frac{\theta_1\,\theta_2}{70} + \frac{L\left(\frac{6\,\theta_2\,w_1}{35} - \frac{6\,\theta_2\,w_2}{35}\right) - \frac{18\,w_1\,w_2}{35} + \frac{9\,{w_1}^2}{35} + \frac{9\,{w_2}^2}{35}}{L^2} + \frac{{\theta_1}^2}{140} - \frac{{\theta_2}^2}{140}, \tag{B.5}$$

$$k_{G,22} = \left(\frac{3\,{w_1}^2}{35} - \frac{6\,w_1\,w_2}{35} + \frac{3\,{w_2}^2}{35}\right)/L - \frac{\theta_1\,w_1}{70} + \frac{\theta_1\,w_2}{70} + \frac{\theta_2\,w_1}{70} - \frac{\theta_2\,w_2}{70} + L\left(\frac{2\,{\theta_1}^2}{35} - \frac{\theta_1\,\theta_2}{70} + \frac{{\theta_2}^2}{210}\right), \tag{B.6}$$

$$k_{G,23} = \frac{{\theta_1}^2}{140} - \frac{L\left(\frac{6\,\theta_1\,w_1}{35} - \frac{6\,\theta_1\,w_2}{35}\right) - \frac{18\,w_1\,w_2}{35} + \frac{9\,{w_1}^2}{35} + \frac{9\,{w_2}^2}{35}}{L^2} - \frac{\theta_1\,\theta_2}{70} - \frac{{\theta_2}^2}{140}, \tag{B.7}$$

$$k_{G,24} = \frac{\theta_1\,w_1}{70} - \frac{\theta_1\,w_2}{70} + \frac{\theta_2\,w_1}{70} - \frac{\theta_2\,w_2}{70} - \frac{L\,{\theta_1}^2}{140} - \frac{L\,{\theta_2}^2}{140} + \frac{L\,\theta_1\,\theta_2}{105}, \tag{B.8}$$

$$k_{G,33} = \left(L\left(\frac{18\,\theta_1\,w_1}{35} - \frac{18\,\theta_1\,w_2}{35} + \frac{18\,\theta_2\,w_1}{35} - \frac{18\,\theta_2\,w_2}{35}\right) - \frac{144\,w_1\,w_2}{35} + L^2\left(\frac{3\,{\theta_1}^2}{35} + \frac{3\,{\theta_2}^2}{35}\right) + \frac{72\,{w_1}^2}{35} + \frac{72\,{w_2}^2}{35}\right)/L^3, \tag{B.9}$$

$$k_{G,34} = \frac{{\theta_2}^2}{140} - \frac{L\left(\frac{6\,\theta_2\,w_1}{35} - \frac{6\,\theta_2\,w_2}{35}\right) - \frac{18\,w_1\,w_2}{35} + \frac{9\,{w_1}^2}{35} + \frac{9\,{w_2}^2}{35}}{L^2} - \frac{{\theta_1}^2}{140} - \frac{\theta_1\,\theta_2}{70}, \tag{B.10}$$

$$k_{G,44} = \left(\frac{3\,{w_1}^2}{35} - \frac{6\,w_1\,w_2}{35} + \frac{3\,{w_2}^2}{35}\right)/L + \frac{\theta_1\,w_1}{70} - \frac{\theta_1\,w_2}{70} - \frac{\theta_2\,w_1}{70} + \frac{\theta_2\,w_2}{70} + L\left(\frac{{\theta_1}^2}{210} - \frac{\theta_1\,\theta_2}{70} + \frac{2\,{\theta_2}^2}{35}\right)', \tag{B.11}$$

with w_1, w_2, θ_1, and θ_2 the nodal displacements defined in Fig. 2.

Data availability

No data was used for the research described in the article.

References

Adhikari, S., 2021. Exact transcendental stiffness matrices of general beam–columns embedded in elastic mediums. Comput. Struct. 255, 106617. http://dx.doi.org/10.1016/j.compstruc.2021.106617.

Adin, M.A., Yankelevsky, D.Z., Eisenberger, M., 1985. Analysis of beams on BI-moduli elastic foundation. Comput. Methods Appl. Mech. Engrg. 49 (3), 319–330. http://dx.doi.org/10.1016/0045-7825(85)90128-8.

Akhazhanov, S.B., Vatin, N.I., Akhmediyev, S., Akhazhanov, T., Khabidolda, O., Nurgoziyeva, A., 2023. Beam on a two-parameter elastic foundation: simplified finite element model. Mag. Civ. Eng. 121 (5), http://dx.doi.org/10.34910/MCE.121.7.

Balabušić, M., Folić, B., Ćorić, S., 2019. Bending the foundation beam on elastic base by two reaction coefficient of Winkler's subgrade. Open J. Civ. Eng. 09 (02), 123–134. http://dx.doi.org/10.4236/ojce.2019.92009.

Ballo, F., Gobbi, M., Mastinu, G., Previati, G., 2016. Motorcycle tire modeling for the study of tire–rim interaction. J. Mech. Des. 138 (5), 051404. http://dx.doi.org/10.1115/1.4032470.

Ballo, F., Gobbi, M., Mastinu, G., Previati, G., Zerboni, R., 2015. Motorcycle tire modeling. In: Proceedings of the ASME Design Engineering Technical Conference, vol. 3, ASME, http://dx.doi.org/10.1115/DETC2015-46607.

Ballo, F., Previati, G., Gobbi, M., Mastinu, G., 2018. Tire-rim interaction, a semi-analytical tire model. J. Mech. Des. 140, 1–12. http://dx.doi.org/10.1115/1.4038927.

Bao, W., Han, H., 1999. The direct method of lines for the problem of infinite elastic foundation. Comput. Methods Appl. Mech. Engrg. 175 (1–2), 157–173. http://dx.doi.org/10.1016/S0045-7825(98)00366-1.

Bekker, M.G., 1969. Off-road locomotion. Ordnance 53 (292), 416–418.

Bowles, J.E., 1974. Analytical and Computer Methods in Foundation Engineering. McGraw-Hill Book Company, Singapore.

Brezzi, F., Fortin, M., 1991. Mixed and Hybrid Finite Element Method. Springer-Verlag, New York, NY, USA.

Chapra, S.C., Canale, R.P., 2009. Numerical Methods for Engineers, sixth ed. Mcgraw-Hill, New York, URL https://linkinghub.elsevier.com/retrieve/pii/C20190046468.

Chen, W.Q., Lü, C.F., Bian, Z.G., 2004. A mixed method for bending and free vibration of beams resting on a Pasternak elastic foundation. Appl. Math. Model. 28 (10), 877–890. http://dx.doi.org/10.1016/j.apm.2004.04.001.

Clastornik, J., Eisenberger, M., Yankelevsky, D.Z., Adin, M.A., 1986. Beams on variable winkler elastic foundation. J. Appl. Mech. Trans. ASME 53 (4), 925–928. http://dx.doi.org/10.1115/1.3171882.

Cojocaru, E.C., Irschik, H., Schlacher, K., 2003. Concentrations of pressure between an elastically supported beam and a moving Timoshenko-Beam. J. Eng. Mech. 129 (9), 1076–1082. http://dx.doi.org/10.1061/(asce)0733-9399(2003)129:9(1076).

Dai, C.Q., Wang, L., Wang, Y.J., 2011. Deformation study of lining on overlap tunnels based on elastic foundation beam. Appl. Mech. Mater. 94–96, 1875–1878. http://dx.doi.org/10.4028/www.scientific.net/AMM.94-96.1875.

Fallah, A., Aghdam, M., 2011. Nonlinear free vibration and post-buckling analysis of functionally graded beams on nonlinear elastic foundation. Eur. J. Mech. A Solids 30 (4), 571–583. http://dx.doi.org/10.1016/j.euromechsol.2011.01.005.

Franklin, J.N., Scott, R.F., 1979. Beam equation with variable foundation coefficient. J. Eng. Mech. Div. 105 (5), 811–827. http://dx.doi.org/10.1061/JMCEA3.0002525, URL https://ascelibrary.org/doi/10.1061/JMCEA3.0002525.

Froio, D., Rizzi, E., 2016. Analytical solution for the elastic bending of beams lying on a variable Winkler support. Acta Mech. 227 (4), 1157–1179. http://dx.doi.org/10.1007/s00707-015-1508-y.

Froio, D., Rizzi, E., 2017. Analytical solution for the elastic bending of beams lying on a linearly variable Winkler support. Int. J. Mech. Sci. 128–129 (March), 680–694. http://dx.doi.org/10.1016/j.ijmecsci.2017.04.021.

Frydrýek, K., Janco, R., Gondek, H., 2013. Solutions of beams, frames and 3 D structures on elastic foundation using FEM. Int. J. Mech. 7 (4), 362–369.

Gao, D.Y., 1996. Nonlinear elastic beam theory with application in contact problems and variational approaches. Mech. Res. Commun. 23 (1), 11–17. http://dx.doi.org/10.1016/0093-6413(95)00071-2.

Gao, D.Y., Machalová, J., Netuka, H., 2015. Mixed finite element solutions to contact problems of nonlinear Gao beam on elastic foundation. Nonlinear Anal. Real World Appl. 22, 537–550. http://dx.doi.org/10.1016/j.nonrwa.2014.09.012.

Girija Vallabhan, C.V., Das, Y.C., 1991. Modified vlasov model for beams on elastic foundations. J. Geotech. Eng. 117 (6), 956–966. http://dx.doi.org/10.1061/(ASCE)0733-9410(1991)117:6(956).

Harden, C.W., Hutchinson, T.C., 2009. Beam-on-nonlinear-winkler-foundation modeling of shallow, rocking-dominated footings. Earthq. Spectra 25 (2), 277–300. http://dx.doi.org/10.1193/1.3110482.

Hetenyi, M., 1946. Beams on Elastic Foundation: Theory with Applications in the Fields of Civil and Mechanical Engineering. The University of Michigan Press, Ann Arbor, Michigan.

Iyengar, K.S.R., Anantharamu, S., 1963. Finite beam-columns on elastic foundations. J. Eng. Mech. Div. 89 (6), 139–160. http://dx.doi.org/10.1061/JMCEA3.0000431, URL https://ascelibrary.org/doi/10.1061/JMCEA3.0000431.

Jain, S., Tiso, P., Haller, G., 2018. Exact nonlinear model reduction for a von Kármán beam: Slow-fast decomposition and spectral submanifolds. J. Sound Vib. 423, 195–211. http://dx.doi.org/10.1016/J.JSV.2018.01.049, arXiv:1703.03001.

Kerr, A.D., 1964. Elastic and viscoelastic foundation models. J. Appl. Mech. Trans. ASME 31 (3), 491–498. http://dx.doi.org/10.1115/1.3629667.

Kim, S., Nikravesh, P.E., Gim, G., 2008. A two-dimensional tire model on uneven roads for vehicle dynamic simulation. Veh. Syst. Dyn. 46 (10), 913–930. http://dx.doi.org/10.1080/00423110701729994.

Klar, A., Vorster, T.E., Soga, K., Mair, R.J., 2005. Soil-pipe interaction due to tunnelling: Comparison between Winkler and elastic continuum solutions. Geotechnique 55 (6), 461–466. http://dx.doi.org/10.1680/geot.2005.55.6.461.

Lamprea-Pineda, A.C., Connolly, D.P., Hussein, M.F., 2022. Beams on elastic foundations – A review of railway applications and solutions. Transp. Geotech. 33 (2021), 100696. http://dx.doi.org/10.1016/j.trgeo.2021.100696.

Liang, F., Li, Y., Li, L., Wang, J., 2014. Analytical solution for laterally loaded long piles based on Fourier-Laplace integral. Appl. Math. Model. 38 (21–22), 5198–5216. http://dx.doi.org/10.1016/j.apm.2014.03.052.

Machalová, J., Netuka, H., 2011a. Bending of a nonlinear beam reposing on an unilateral foundation. Appl. Comput. Mech. 5, 45–54.

Machalová, J., Netuka, H., 2011b. Solving the beam bending problem with an unilateral Winkler foundation. AIP Conf. Proc. 1389, 1820–1824. http://dx.doi.org/10.1063/1.3636963.

Machalová, J., Netuka, H., 2015. Solution of contact problems for nonlinear Gao beam and obstacle. J. Appl. Math. 23, 1–12. http://dx.doi.org/10.1177/1081286517732382.

Machalová, J., Netuka, H., 2017. Control variational method approach to bending and contact problems for Gao beam. Appl. Math. 62 (6), 661–677. http://dx.doi.org/10.21136/AM.2017.0168-17.

Machalová, J., Netuka, H., 2018. Solution of contact problems for Gao beam and elastic foundation. Math. Mech. Solids 23 (3), 473–488. http://dx.doi.org/10.1177/1081286517732382.

Madhira, M., Abhishek, S.V., Rajyalakshmi, K., 2016. Modelling ground-foundation interactions. In: International Conference on Innovations in Structural Engineering. Hyderabad, India, pp. 91–106.

Malekzadeh, P., Karami, G., 2008. A mixed differential quadrature and finite element free vibration and buckling analysis of thick beams on two-parameter elastic foundations. Appl. Math. Model. 32 (7), 1381–1394. http://dx.doi.org/10.1016/j.apm.2007.04.019.

Malik, A.S., Grandhi, R.V., 2008. A computational method to predict strip profile in rolling mills. J. Mater. Process. Technol. 206 (1–3), 263–274. http://dx.doi.org/10.1016/j.jmatprotec.2007.12.026.

Mourelatos, Z.P., Parsons, M.G., 1987. A finite element analysis of beams on elastic foundation including shear and axial effects. Comput. Struct. 27 (3), 323–331. http://dx.doi.org/10.1016/0045-7949(87)90055-1.

Onu, G., 2008. Finite elements on generalized elastic foundation in Timoshenko beam theory. J. Eng. Mech. 134 (9), 763–776. http://dx.doi.org/10.1061/(ASCE)0733-9399(2008)134:9(763).

Pasternak, P.L., 1954. On a new method of analysis of an elastic foundation by means of two foundation constants. In: Gosudarstvennoe Izdatelstro Liberaturi Po Stroitelstvui Arkhitekture. Moscow.

Radová, J., Machalová, J., 2024. Parameter identification in contact problems for Gao beam. Nonlinear Anal. Real World Appl. 77 (2023), 104068. http://dx.doi.org/10.1016/j.nonrwa.2024.104068.

Singh, H., Jha, J.N., 2013. Constitutive models for sustainable design of foundation systems. In: UKIERI Concrete Congress - Innovations in Concrete Construction. May.

Tiwari, K., Kuppa, R., 2014. Overview of methods of analysis of beams on elastic foundation. IOSR J. Mech. Civ. Eng. 11 (5), 22–29. http://dx.doi.org/10.9790/1684-11562229.

Wang, Y.H., Tham, L.G., Cheung, Y.K., 2005. Beams and plates on elastic foundations: A review. Progress Struct. Eng. Mater. 7 (4), 174–182. http://dx.doi.org/10.1002/pse.202.

Winkler, E., 1868. Die lehre von der elastizität und festigkeit, no. v. 1 in die lehre von der elastizität und festigkeit mit besonderer rücksicht auf ihre anwendung in der technik: für polytechnische schulen, bauakademien, ingenieure, maschinenbauer, architecten, etc, dominicus, prag.

Xiong, Z., Kou, L., Zhao, J., Cui, H., Wang, B., 2023. Isogeometric analysis of longitudinal displacement of a simplified tunnel model based on elastic foundation beam. CMES - Comput. Model. Eng. Sci. 136 (1), 803–824. http://dx.doi.org/10.32604/cmes.2023.024833.

Younesian, D., Hosseinkhani, A., Askari, H., Esmailzadeh, E., 2019. Elastic and viscoelastic foundations: a review on linear and nonlinear vibration modeling and applications. Nonlinear Dynam. 97 (1), 853–895. http://dx.doi.org/10.1007/s11071-019-04977-9.

Zhang, S., Fan, W., 2023. An exact spectral formulation for the wave characteristics in an infinite Timoshenko-Ehrenfest beam supported by periodic elastic foundations. Comput. Struct. 286, 107105. http://dx.doi.org/10.1016/j.compstruc.2023.107105.

Zhang, Y., Liu, X., Wei, Y., 2018. Response of an infinite beam on a bilinear elastic foundation: Bridging the gap between the Winkler and tensionless foundation models. Eur. J. Mech. A Solids 71, 394–403. http://dx.doi.org/10.1016/j.euromechsol.2018.06.006.

Zhang, F., Malik, A., 2018. A roll-stack contact mechanics model to predict strip profile in rolling mills with asymmetric, continuously variable crown rolls. Trans. ASME, J. Manuf. Sci. Eng. 140 (1), http://dx.doi.org/10.1115/1.4037600.

Zhang, Y., Murphy, K.D., 2004. Response of a finite beam in contact with a tensionless foundation under symmetric and asymmetric loading. Int. J. Solids Struct. 41 (24–25), 6745–6758. http://dx.doi.org/10.1016/j.ijsolstr.2004.05.028.

Zhang, Y., Murphy, K.D., 2013. Tensionless contact of a finite beam: Concentrated load inside and outside the contact zone. Acta Mech. Sin. 29 (6), 836–839. http://dx.doi.org/10.1007/s10409-013-0081-7.

Zhang, Y., Zhao, Y.P., 2012. Flexural contact in MEMS stiction. Int. J. Solids Struct. 49 (17), 2203–2214. http://dx.doi.org/10.1016/j.ijsolstr.2012.03.032.

Zhaohua, F., Cook, R.D., 1983. Beam elements on two-parameter elastic foundations. J. Eng. Mech. 109 (6), 1390–1402. http://dx.doi.org/10.1061/(asce)0733-9399(1983)109:6(1390).